CHROMSYMP. 2469

Adsorption kinetics of albumin on a cross-linked cellulose chromatographic ion exchanger

G. Leaver☆, J. A. Howell☆☆ and J. R. Conder*

Chemical Engineering Department, University of Wales, Swansea SA2 8PP (UK)

ABSTRACT

Cross-linked, regenerated cellulose offers faster separation of proteins than softer gels can achieve. The kinetics of adsorption of bovine serum albumin have been studied on a Vistec granular DEAE-cellulose. A differential bed technique has been applied to proteins for the first time and allows results to be obtained more rapidly than with a larger bed. The dependence of the adsorption rate on the superficial flow velocity, salt concentration and protein concentration is examined. Although salt and protein compete strongly for adsorption sites the initial rate of adsorption is insensitive to salt concentration but sensitive to protein concentration. The rate-determining step in adsorption appears to be predominantly diffusion within the pores of the particles. Two single-step models of the kinetics have been developed: a pore diffusion model predicts the breakthrough curves better than a lumped mass transfer model, but a two-step model is likely to give better predictive accuracy than either. Some guiding principles are derived for optimising protein throughput.

INTRODUCTION

The largest part of the production costs of new biotechnology products usually arises in downstream processing. Processing sequences increasingly use chromatographic separation stages. Two important processes in which chromatographic stages have recently been introduced are the separation of blood proteins from animal and human blood.

Large quantities of valuable protein, in the form of animal blood from abattoirs and poultry processing, are currently wasted as process effluent [1]. The protein in blood can be separated from non-proteins by ion-exchange adsorption and desorption [2,3]; a protein powder produced in this way is now on the market for use in food mixes. The value of blood proteins, however, can be greatly increased if they are fractionated into specific proteins such as albumin [4]. This protein accounts for half the protein content of blood and its recovery is a potentially high tonnage process.

For fractionation of human blood proteins the classical alcohol precipitation techniques of Cohn and co-workers [5,6] are still dominant. In recent years, one of the most significant modifications to the Cohn process has been the incorporation of ion-exchange separation stages. New separation protocols have been devised based on ion-exchange, affinity or size-exclusion chromatography [7–14]. Production chromatography of proteins [15] and the relative merits of different forms of the technique [16] have been reviewed. Much of the literature is concerned with qualitative descriptions of the process; there is little information on the effect of process variables on performance for affinity chromatography [17–20] and even less for ion-exchange chromatography [21,22].

In order to design a chromatographic process to purify proteins, it is important to be able to predict the performance as a function of the operating conditions. We have recently studied the effect of operating conditions on the separation of albumin from bovine serum on a Vistec diethylaminoethyl (DEAE) cellulose ion exchanger [16]. The Vistec

---

☆ Present address: Warren Spring Laboratory, Gunnels Wood Road, Stevenage, Herts. SG1 2BX, UK.
☆☆ Present address: Chemical Engineering Department, University of Bath, Claverton Down, Bath BA2 7AY, UK.

medium is a cross-linked, regenerated cellulose which provides an improved adsorbent matrix for the chromatographic separation of proteins [23]. Optimal operation was shown to require trade-offs between the major operating variables such as feed band width, feed dilution, eluent velocity, column length and packing rigidity [16]. A better understanding of the way in which the process variables determine performance can be gained by studying their influence on the process equilibria and adsorption kinetics directly. We have recently reported an investigation of the equilibria of adsorption of bovine serum albumin (BSA) on the Vistec ion-exchanger [23]. Here we describe a study of the adsorption kinetics of the same process. The first part of this study concerns the effect of process variables on the kinetics. In the final part a simplified kinetic model is developed and validated to permit prediction of breakthrough curves.

EXPERIMENTAL METHOD

Adsorption kinetics are often studied by using a stirred vessel but this method has only limited applicability: if there is significant extra-particle resistance to mass transfer the kinetics depend on the mixing pattern and differ from those in a packed bed. A packed bed technique is better suited to obtaining kinetic data that are to be used in designing packed columns. (A further advantage of the packed bed approach is described below.) We have adopted a variant of the packed bed technique that uses a very short "differential" bed. The technique was originally devised by Tien and Thodos [24] to study the adsorption of oxalic acid and allows results to be obtained more rapidly than with a longer bed.

The packed column was 15 mm high × 76 mm in diameter, giving an empty column volume (ECV) of 68 ml. With such a short bed it is important to achieve a uniform flow distribution over the cross-section. The column was constructed from QVF glass tubing and Corning flange pieces. Polypropylene end-plates with a central tapped hole for the liquid inlet or outlet (and, in the case of the inlet plate, a second tapped hole for a pressure gauge) were separated by a shallow (ca. 2 mm) chamber from an 8-hole flow distributor, in turn separated from a coarse (ca. 80 μm) mesh and 10 mm thick

stainless-steel sinter retaining the packing. This arrangement produced a good distribution of liquid flow over the cross-section. The direction of flow was downward.

The materials were as previously described [23]. The D2 grade of Vistec DEAE-cellulose medium was used throughout. The particle size was determined to be 192 ± 36 μm by 242 ± 78 μm. BSA was made up in Tris buffer with sodium chloride added to the desired ionic concentration [23].

At the start of each run water was passed through the bed. When the conductivity was about $20 \cdot 10^{-6}$ S the feed was switched to albumin solution of the desired concentration and ionic strength. Conductivity and pH were continuously monitored at the outlet of the bed. The protein breakthrough curve was monitored with a Pye UV20 continuous detector at a wavelength of 280 nm. This detector, however, was insensitive to concentration change at high protein concentrations. Samples were therefore taken from the detector exit and analysed on a Pye SP6UV spectrophotometer at 280 nm to measure the concentration at specific points on the breakthrough curve. When the run was complete the bed was regenerated in accord with the manufacturer's literature, by switching the feed to water, then 0.2 M salt solution to desorb the protein, and finally water again. Subsequent measurements showed that a minimum salt concentration of 0.26 M would be required to desorb protein completely [23]. All protein concentrations reported in this paper (including simulations, which use experimental data) are therefore nominal and must be increased by 0.12 kg/kg dry medium to give true concentrations.

The adsorption kinetics were studied by following the progress of the breakthrough curve, which is a plot of the protein concentration c_o in the liquid eluting from the column outlet against time elapsed after a concentration step change from $c = 0$ to $c = c_f$ is introduced at the inlet. The mean concentration q of protein adsorbed on the solid at any point P on the breakthrough curve is obtained by a mass balance, i.e., by subtracting the sum of (i) the mass of protein eluted from the column up to point P and (ii) the mass of protein in the liquid holdup (in the bed, column end pieces and connecting tubing) from the mass fed to the column and dividing by the dry mass W of the ion exchanger. Thus,

$$q = \frac{F}{W} \left[\int_0^t (c_f - c_o) \, dt - c_f t_M \right] \qquad (1)$$

where F is the volumetric flow-rate and t_M is the liquid holdup time in the bed. t_M was determined by switching the feed stream to water, which does not desorb protein.

EXPERIMENTAL RESULTS AND DISCUSSION

Establishing the differential bed method

The mean protein concentration in the solid phase q is shown as a function of ECVs passed in Fig. 1. The breakthrough curves from which these plots are derived started together at 1.8 ± 0.2 ECV, which barely exceeds the liquid holdup (1.65 ECV). This is good evidence that the bed is acting as a true differential bed. Confirmation comes from the shape of the breakthrough curve. The present adsorption system has an isotherm with Langmuir-type curvature, concave towards the mobile phase concentration axis [23]. A bed long enough to contain several theoretical plates would therefore give a breakthrough curve which would start at a time later than t_M and develop rapidly through a steep, sigmoid form to early completion, i.e., the migrating frontal boundary would be of the constant-pattern self-sharpening type [25]. The fact that the progress of

breakthrough here occupies many column volumes confirms that the bed is of "differential" length.

Effect of superficial velocity

A comparison of Fig. 1 and the adsorption isotherms [23] for corresponding operating conditions shows that equilibrium is not established within the several minutes of the transient study. For example, at an ionic concentration of 5 kg/m^3, a liquid phase protein concentration of 5 kg/m^3 would produce an equilibrium solid concentration of 0.52 kg/kg but nominal values of only 0.11–0.19 kg/kg, corresponding to a true 0.23–0.31 kg/kg, are reached in Fig. 1. Part of this difference is due to the use of virgin medium for each equilibrium isotherm point as against bed regeneration in the kinetic studies. Even so, complete attainment of equilibrium appears to require times of the order of a few hours rather than a few minutes. The influence of slow adsorption kinetics is confirmed by the evidence in Fig. 1 that, in terms of column volumes passed, breakthrough develops more slowly at higher velocities.

Fig. 2 shows the same data as Fig. 1 replotted with time instead of ECV as abscissa. The order of the curves for different velocities is reversed. This is as expected for a differential bed if the adsorption rate is controlled more by the kinetics of mass transfer
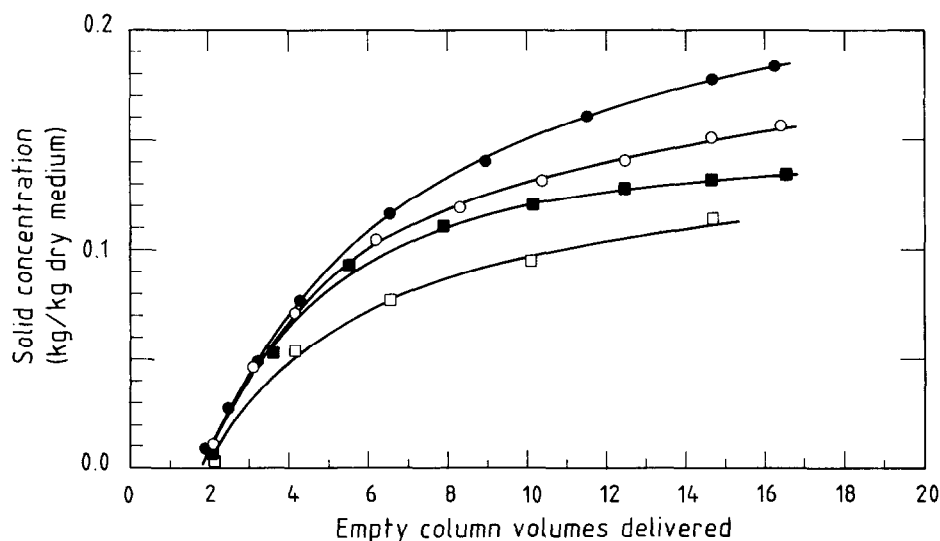

Fig. 1. Effect of superficial velocity u on protein breakthrough curve for ionic concentration (NaCl) 5 kg/m^3, pH 7.5, $c_f = 5$ kg/m^3. u: ● = 0.06 mm/s; ○ = 0.13 mm/s; ■ = 0.28 mm/s; □ = 0.86 mm/s.
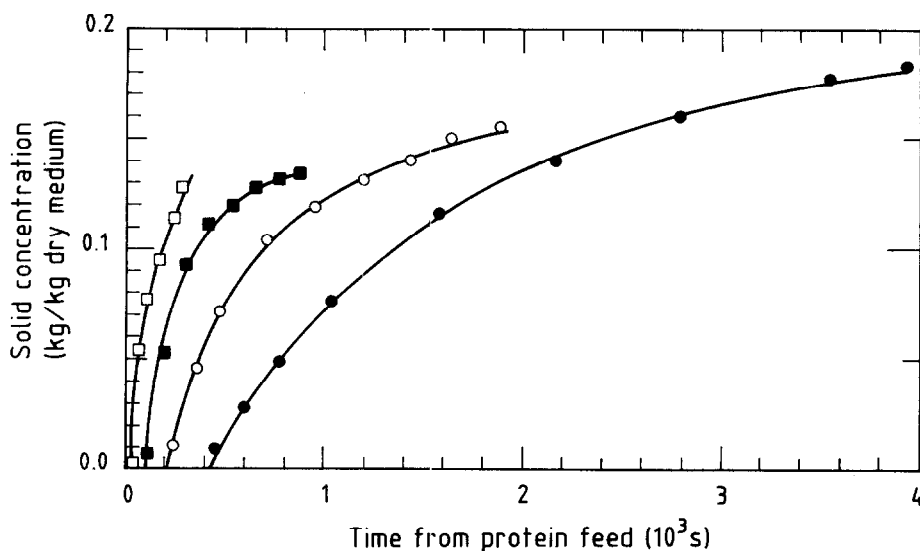
Fig. 2. As Fig. 1 but with abscissa expressed as time from step change in protein feed concentration to c_f at column inlet. Symbols as in Fig. 1.

within the particles (*e.g.*, by pore diffusion) than that through the liquid "film" outside the particles.

From a practical point of view, a low velocity has the advantage of achieving a given adsorbed concentration with least wastage of protein in the effluent (Fig. 1). On the other hand, it is seen from Fig. 2

that, where cycle time is more important than wastage, a high velocity gives a faster increase in the amount of protein adsorbed.

Effect of ionic concentration
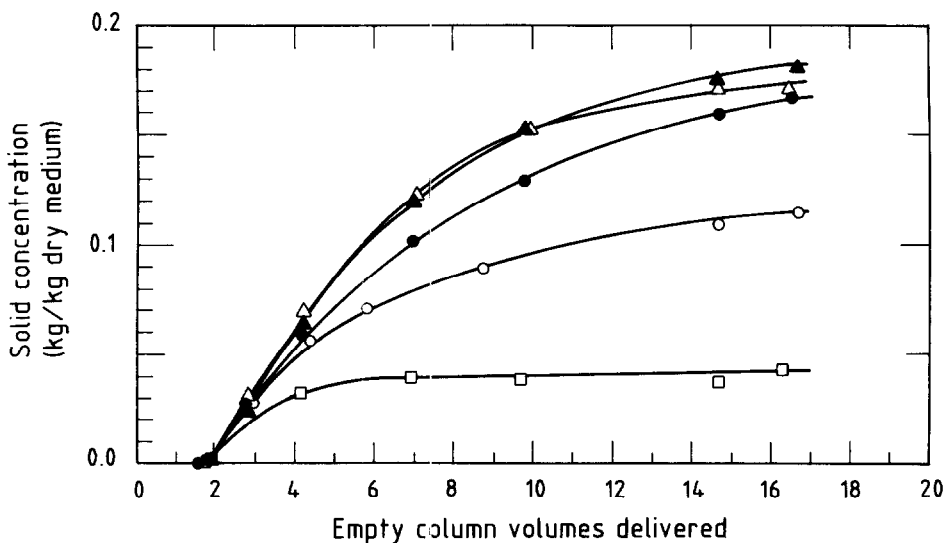
Fig. 3 shows the effect of ionic concentration on

Fig. 3. Effect of ionic concentration I (kg $NaCl/m^3$) on breakthrough curve at pH 7.5, $c_f = 5$ kg/m^3, superficial velocity 0.37 mm/s. I: ▲ = 0 kg/m^3; △ = 1 kg/m^3; ● = 3 kg/m^3; ○ = 5 kg/m^3; □ = 10 kg/m^3.

the progress of adsorption. Initially, the rate of adsorption is not very sensitive to the ionic concentration. As equilibrium is approached, however, the adsorption rate becomes more sensitive to ionic concentration; this behaviour reflects the pattern of the adsorption isotherms previously reported [23] in that the adsorbed concentration at equilibrium decreases as the ionic concentration in the feed increases. The change in sensitivity to ionic concentration probably reflects a change from transport-limited to thermodynamic-limited control of the kinetics. The initial adsorption rate is controlled by mass transfer through the liquid film and internal pores. Subsequently the important factor becomes competition with other ions for sites on the ion exchanger surface.

There are two other notable differences between equilibrium and transient behaviour. First, reduction of the ionic concentration within the range 0–5 kg/m^3 significantly improves the rate of adsorption seen in Fig. 3, but has no beneficial effect on the equilibrium uptake of protein previously reported [23]. The equilibrium uptake increases with decreasing ionic concentrations down to 5 kg/m^3 but varies little at lower ionic concentrations (so long as the ratio of salt to protein concentrations is maintained above 20).

Secondly, in the batch (equilibrium) studies it is necessary to use high initial concentrations of protein in the liquid phase to achieve a given final uptake. At low ionic concentrations this creates a risk of agglomeration of the protein molecules. The problem does not arise in the continuous flow process: the protein feed concentration is the same at the beginning and end of the process. Even at zero concentration of added salt, sufficient salts are present in the buffer solution of the feed to maintain the protein/salt concentration below its critical value [23] of 20 and the protein remains unagglomerated.

Effect of protein feed concentration

Fig. 4 shows the effect of varying the protein feed concentration c_f at a constant ionic concentration of 3 kg/m^3. The non-linear relationship between protein uptake and feed concentration for a given volume of eluate passed is as expected from the isotherm, which is of the Langmuir type [23]. Because the relationship is non-linear, higher protein uptake is achieved only at the cost of a greater proportional loss of protein in the eluent stream.

The initial rate of adsorption is more sensitive than the later rate to protein feed concentration, *i.e.*, the proportion of the equilibrium solid concentration achieved at any given time less than infinite time
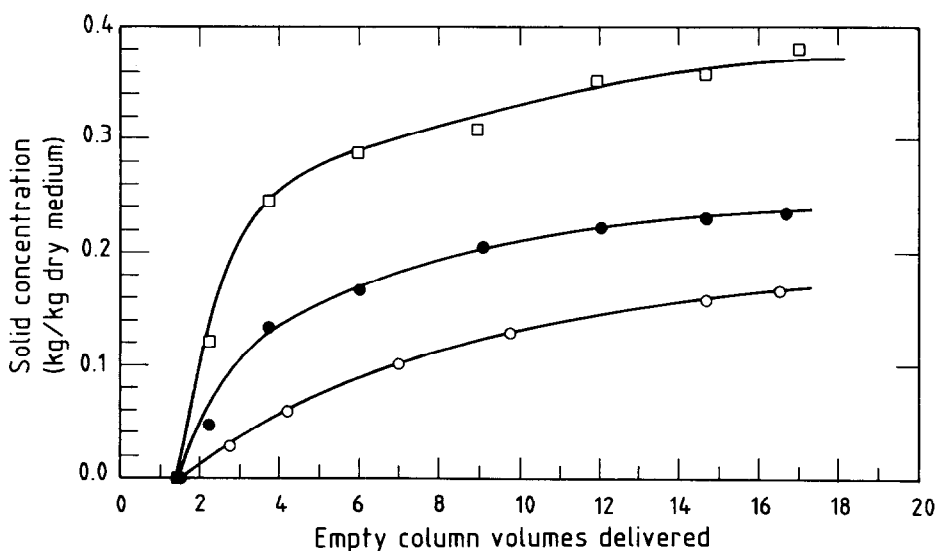

Fig. 4. Effect of protein feed concentration c_f on breakthrough curve at pH 7.5, ionic concentration (NaCl) 5 kg/m^3, superficial velocity 0.37 mm/s. c_f: □ = 25 kg/m^3; ● = 10 kg/m^3; ○ = 5 kg/m^3.

is higher for higher protein feed concentrations. This finding is important for optimising the performance of the chromatographic separation of proteins because it implies that the protein feed should be introduced at as high a concentration as possible. For example, passing 20 ECVs of feed of concentration 5 kg/m^3 would produce an adsorbed concentration of about 0.17 kg/kg. The same mass of protein fed at a concentration of 10 kg/m^3 in a feed band of 10 ECVs would raise the adsorbed concentration to 0.21 kg/kg. The faster adsorption achieved by doubling the protein concentration outweighs the halving of available contact time. This conclusion applies only if the salt concentration exceeds 5 kg/m^3 and if the volume of feed is concentrated without change in the salt concentration. In practice, simple concentration or dilution of feed will change the concentration, not only of protein but also of salt.

Dilution: combined effects of ionic and protein concentrations

Fig. 5 demonstrates the effect of combining two different protein concentrations with two ionic concentrations.

As expected, there are two regimes of behaviour depending on contact time. The initial adsorption

rate (low contact times, solid concentration much less than equilibrium value) is largely unaffected by ionic concentration but is more sensitive than the later rate to protein feed concentration. The later adsorption rate, corresponding to high contact times where the solid concentration is a substantial fraction of the equilibrium value, is affected by both ionic and protein concentrations.

The effect of feed dilution is seen by comparing curves 2 and 3. Curve 3 was obtained by diluting, to a five times greater volume, a protein feed similar to that of curve 2. Despite the lower protein concentration in diluted feed, the combined effects of lower ionic concentration and greater adsorption time (in the sense of a greater volume of more dilute feed delivered) give a three times greater uptake of protein on completion of delivery. In the earliest stages of delivery, however, the undiluted feed gives the greater uptake. Thus, the effective capacity of the ion exchanger for protein generally increases with dilution unless contact times are short. This is consonant with the chromatographic findings [16].

MODELLING THE ADSORPTION KINETICS

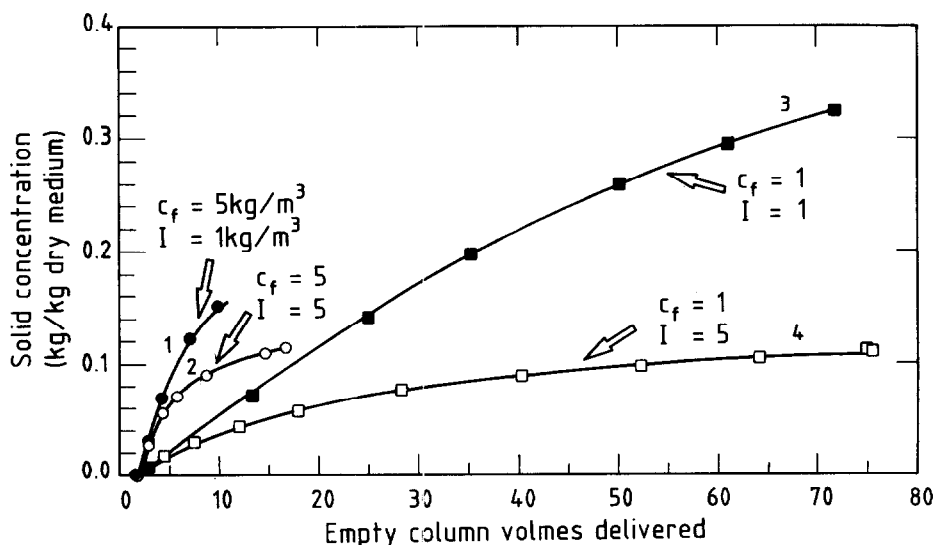Models of protein adsorption in packed beds

Fig. 5. Effect of protein concentration c_f and ionic concentration I at pH 7.5, superficial velocity 0.37 mm/s.

[17,20–22,26–28] differ from each other in two main characteristics: the type of equilibrium isotherm, and the nature of the mass transfer resistance to the sorption process.

Protein adsorption isotherms are usually found to be favourable, *i.e.*, concave to the liquid concentration axis. The Langmuir isotherm, which is of this type, can be theoretically justified for proteins [23]. It relates q and c, the concentrations in the solid and liquid phases, respectively, at equilibrium:

$$q = \frac{K_m q_m c}{1 + K_m c} \qquad (2)$$

q_m is the adsorbent capacity and K_m (the ratio of the adsorption and desorption rate constants) determines the curvature of the isotherm. Previous models of protein adsorption have sometimes been based on a linear or rectangular ("irreversible") isotherm [20,27]. These can be regarded as extreme cases of a Langmuir isotherm, with K_m equal to 0 or ∞, respectively. Since the isotherm has a major effect on the model breakthrough curve we have instead adopted the normal (finite K_m) Langmuir isotherm which fits BSA adsorption on Vistec well [23].

Adsorption into porous particles is assumed to proceed in a series of steps: (i) diffusion through the liquid film external to the particle, (ii) diffusion through liquid held in pores of the particle, and (iii) the surface reaction at the liquid–solid interface. Surface diffusion in parallel with pore diffusion [29] is not likely to be significant for proteins. It is assumed that step (iii), surface reaction, is not rate-limiting. This agrees with a recent affinity adsorption study [26]. The simplest modelling approach is to lump the steps together and describe the adsorption rate by a single term involving a lumped mass transfer coefficient. Such a model can also encompass the case where transfer across the liquid film is rate-limiting since the rate expressions have the same mathematical form. The alternative limiting case is that pore diffusion, rather than the liquid film, is rate-limiting. The experimental evidence so far described indicates that both pore diffusion and the liquid film may determine the rate of adsorption, but that pore diffusion may be dominant. A model based on one of these processes alone is simpler and makes less demands on computer time and storage. We have therefore sought to compare two versions of the model, one based on a lumped mass transfer resistance and the other on pore diffusion. An analytical solution exists for the lumped mass transfer model [30] but we have developed a numerical solution in parallel with the pore diffusion model for comparability.

In both models it is additionally assumed that (i) axial dispersion is negligible in the packed bed, (ii) the particles are spherical and of uniform size, density and porosity, and (iii) ion-exchange groups are uniformly distributed throughout each particle. There is evidence that assumptions (ii) and (iii) are reasonably well satisfied for the D2 grade of Vistec used here [23]. In addition, since protein concentrations are small, volume changes in the liquid and diffusion-induced convection in particle pores are neglected.

Model development

The basis of a packed bed adsorption model is a mass balance for the adsorbate in the fluid phase in the voids external to the particle. Two approaches are available. The mass balance may be based either on an element of the packed bed [31] or on an element of the moving liquid. We have adopted the second approach.

The column is divided up lengthwise into a number n_c of sections short enough for the protein concentrations to be regarded as uniform within each section. At zero time the protein concentration in the inter-particle liquid in the first section is raised from zero to c_f and thereafter maintained at that value. During the time that the first elemental volume of protein solution remains in the first section it loses some protein by adsorption into the packing. The depleted liquid then passes into the second column section and is further depleted of protein. In general, when an elemental volume of liquid $\varepsilon \Delta v$ passes from section l to section $(l + 1)$, it is depleted of protein according to the mass balance equation

$$c_{l+1} = c_l - \frac{R \Delta t}{\varepsilon \Delta v} \qquad (3)$$

where R is the rate of transfer of protein into the adsorbent particles in section l, calculated from the appropriate rate equation given below, and Δt is the time increment

$$\Delta t = \frac{\varepsilon \Delta v}{F} \qquad (4)$$

(Symbols are defined at the end of the paper.) The value of c_{l+1} so calculated is the protein concentration in the liquid phase presented to the next column section as the elemental volume of liquid progresses along the column.

The scheme is to start at zero time at the column inlet and calculate c_2 from c_1 ($= c_f$). l is incremented to scan the progress of the first liquid element from inlet to outlet of the column. After each scan, time is incremented at the column inlet by Δt and the scan is repeated. The data-pair t and c_l at the column outlet where $l = n_c + 1$ are recorded at regular time intervals to give the breakthrough curve.

Rate equation for lumped mass transfer resistance

The increment in the mean concentration of protein in the solid phase of the adsorbent in column section l in time Δt can be expressed as

$$\Delta q = k(c_l - c^*)\Delta t \qquad (5)$$

where c^*, the liquid concentration in the intra-particle pores in equilibrium with q, is calculated from the current value of q via the Langmuir isotherm eqn. 2. The new value of q is calculated by adding Δq to the current value and the new c^* is derived. The desired rate term is then given by

$$R\Delta t = \Delta v(\phi \Delta c^* + G\Delta q) \qquad (6)$$

Rate equation for pore diffusion resistance

Consider a spherical surface of radius r within a spherical, porous particle. The fraction of the spherical surface occupied by pores is taken to be the same as the fraction of particle volume occupied by pores, i.e., $\phi/(1 - \varepsilon)$ [31]. A mass balance on protein diffusing through the pore-occupied fraction of the spherical surface leads to the equation

$$\frac{\mathscr{D}}{r^2} \frac{\partial}{\partial r}\left(r^2 \frac{\partial c}{\partial r}\right) = \frac{\partial c}{\partial t} + \frac{G}{\phi} \frac{\partial q}{\partial t} \qquad (7)$$

Substituting for $\partial q/\partial c$ from eqn. 2, we obtain

$$\frac{\partial c}{\partial t} = \frac{\mathscr{D}}{1 + \dfrac{G}{\phi} \cdot \dfrac{q_m K_m}{(1 + K_m c)^2}}\left[\frac{\partial^2 c}{\partial r^2} + \frac{2}{r} \cdot \frac{\partial c}{\partial r}\right] \qquad (8)$$

The partial differential equation is solved numerically with an explicit form of computational molecule. Using a first order forward difference formula

for $\partial c/\partial t$ and $\partial c/\partial r$ and a second order central difference formula for $\partial^2 c/\partial r^2$, we obtain

$$c_i^{j+1} = c_i^j + \frac{\mathscr{D}\Delta t}{1 + \dfrac{G}{\phi} \cdot \dfrac{q_m K_m}{(1 + K_m c)^2}} \cdot$$
$$\left[\frac{c_{i+1}^j - 2c_i^j + c_{i-1}^j}{(\Delta y)^2} - \frac{2(c_{i+1}^j - c_i^j)}{\Delta y\left(\dfrac{d_p}{2} - y\right)}\right] \qquad (9)$$

where i is the distance counter along the pore and j is the time counter.

The boundary conditions are

$$c_1^j = c_l, \quad j \geqslant 1$$
$$c_i^1 = 0, \quad i = 2 \text{ to } n \qquad (10)$$
$$\partial c/\partial y = 0, \quad y = d_p/2$$

Eqn. 9 permits the new concentration profile of protein along a pore (i.e., a set of c_i for $i = 1$ to n) after a time increment Δt to be calculated from the previous pore profile by repeated application of eqn. 9. The mass transfer rate R is then obtained from the concentration gradient at the mouth of the pore by the equation

$$R = \frac{\mathscr{D}s}{\Delta y}(c_l - c_2^j) \qquad (11)$$

where s, the total area of pore mouth in an elemental section Δv of the column, is given by

$$s = 6\phi \Delta v/d_p \qquad (12)$$

RESULTS OF THE SIMULATION

Breakthrough curves have been simulated using both the lumped mass transfer and pore diffusion versions of the model and compared with experimental data. The simulations were performed with the 15 mm long differential bed divided into 15 elemental sections and with parameter values $G = 154$ kg/m^3, $G/\phi = 380$ kg/m^3, $d_p = 200$ μm, $u = 3.65 \cdot 10^{-4}$ m/s, $c_f = 5$ kg/m^3, $I = 5$ kg/m^3, pH 7.5, and $q_m = 0.42$. For the pore diffusion model the pore length, $d_p/2$, was divided into $n = 20$ sections, the minimum number below which the breakthrough curve became dependent on n. The numerical computation schemes showed no sign of instability over the range of variables used.
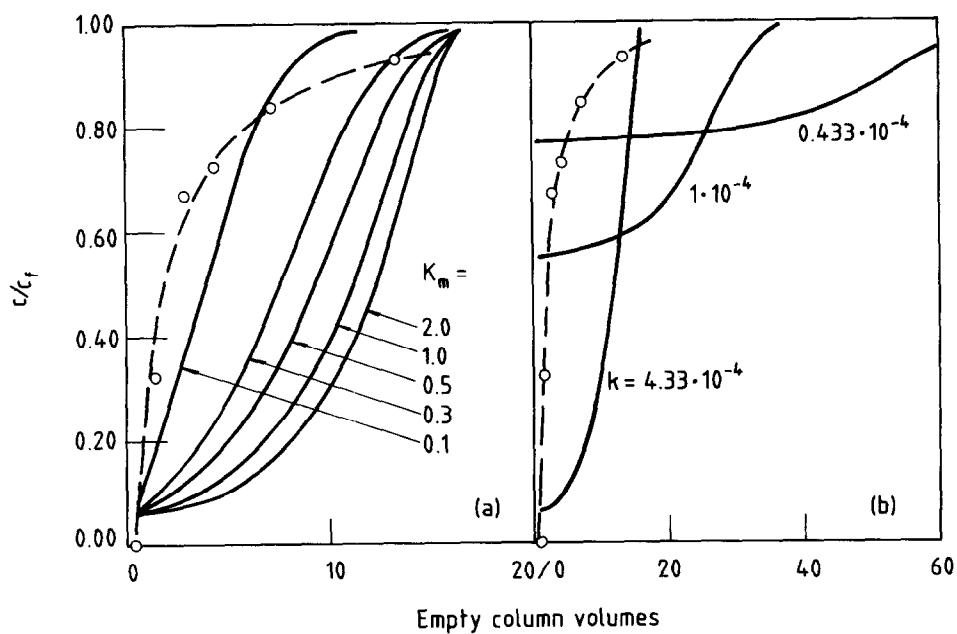
Fig. 6. Simulated breakthrough curves using lumped mass transfer model. (a) Effect of Langmuir constant K_m/m^3 kg^{-1} with $k = 4.33 \cdot 10^{-4}$ $m^3/(kg\ s)$. (b) Effect of mass transfer coefficient k/m^3 $(kg\ s)^{-1}$ with $K_m = 2$ m^3/kg. The broken curves are experimental.
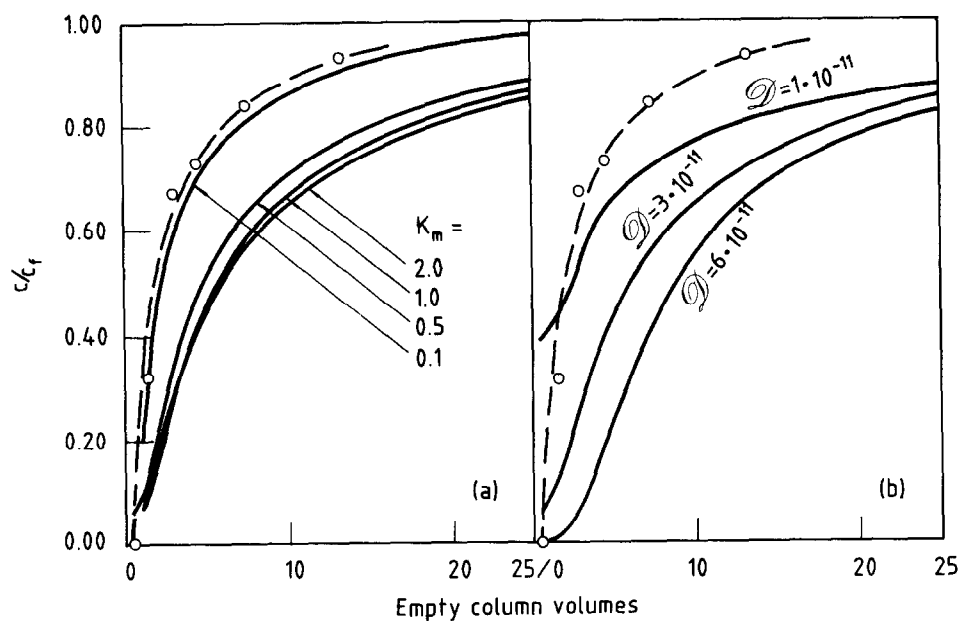

Fig. 7. Simulated breakthrough curves using pore diffusion model. (a) Effect of Langmuir constant K_m with $\mathscr{D} = 3 \cdot 10^{-11}$ m^2 s^{-1}. (b) Effect of diffusivity $\mathscr{D}/m^3$ s^{-1} with $K_m = 2$ m^3/kg. The broken curves are experimental.

The sensitivity of the two models to the Langmuir isotherm's non-linearity parameter K_m is shown in Figs. 6a and 7a. The sensitivity increases rapidly as K_m falls, as anticipated from eqn. 2. It is evident that models based on the simplifying assumption of a linear ($K_m \rightarrow 0$) or rectangular ($K_m \rightarrow \infty$) isotherm will give very different results and are unlikely to be satisfactory. Particularly noteworthy is the way the lumped mass transfer breakthrough curves change shape as K_m varies and tend to converge at high degrees of breakthrough.

Figs. 6b and 7b show that at low values of their respective rate parameter (k or $\mathscr{D}$) both models predict breakthrough curves starting at high values of protein concentration. The rate at which the curves develop subsequently, however, is more sensitive to the lumped mass transfer coefficient than to pore diffusivity. The curves in Fig. 7b cross above 30 ECV.

An experimental breakthrough plot is shown in Figs. 6 and 7 for the same conditions as the simulated curves. The Langmuir parameter K_m to be associated with the experimental plot lies between 0.5 and 2.0 m^3/kg. The range reflects irreproducibility in the regenerated medium but is not as wide as it seems since both the Langmuir isotherm and the simulated breakthrough curves are insensitive to K_m at these (large) values of K_m. Only one parameter, k or $\mathscr{D}$, is to be obtained by fitting the simulated curves to the experimental data. It is evident from Figs. 6 and 7 that neither model provides a very good fit. However, the exponentially shaped breakthrough curves of the pore diffusion model accord better with the experimental shape than do the generally sigmoid-shaped curves of the lumped mass transfer model. This is consistent with the earlier conclusion that pore diffusion offers a larger resistance than external film transport. Examination of Figs. 6 and 7 indicates that a two-step model in which a pore diffusion resistance is combined with an external resistance would be likely to bring the curves into closer alignment with experiment, as has been found for an affinity adsorption system [26].

Fig. 7 suggests that the effective pore diffusion coefficient is about $3 \cdot 10^{-11}$ m^2/s. This is half the value of $6.0 \cdot 10^{-11}$ m^2/s predicted by the correlation of Young *et al.* [32] for BSA at 293 K in free solution. The high value of 1/2 in comparison with literature values of 1/20–1/100 [21,22] is probably due mainly to the large pore size of the Vistec medium, which has been estimated at 50–100 nm [33].

CONCLUSIONS

The purpose of studying the adsorption kinetics is to provide a basis for optimising the design and operating conditions of the chromatographic separation. Several guiding principles can be deduced from this study.

Amongst the variables that determine the throughput (processing rate) of protein, those that relate to the adsorption kinetics include superficial velocity, feed volume (band width), protein feed concentration and ionic concentration. Optimisation will involve trade-offs between these variables.

If the feed is dialysed before it is chromatographed, the protein concentration and ionic concentration can be controlled independently to maximise adsorption. This benefit is offset by the extra cost, and possibly time, consumed by the extra unit operation of dialysis. If the feed is not dialysed, the two concentrations are coupled. Dilution may then be a beneficial tactic. It increases the effective adsorption capacity unless the feed band width, and hence contact time, is abnormally small. With a normal column of, say, 0.3 m length, as opposed to a differential bed, even 0.03 ECV of bovine plasma is in the range where the effective capacity improves with dilution [16]. The overall effect on the protein throughput, however, also depends on how much the overall cycle time has to be raised to process the larger volume of diluted feed.

As the liquid velocity is increased, the bed contact time available for protein adsorption decreases. This is partly counteracted by an increase in the adsorption rate to an extent depending on the nature of the controlling mass transfer resistance. The net result is some fall in the effective adsorption capacity of the bed. The fall is found to be small for the BSA + Vistec system under chromatographic process conditions [16]. Liquid velocity then controls protein throughput more through the cycle time than through the effective capacity, and the throughput increases almost linearly with velocity.

Since the mass transfer kinetics are largely controlled by pore diffusion, the use of smaller particles will increase the rates of adsorption and desorption. With a compressible medium, however, reduced

particle size can be achieved only at the expense of reduced velocity and the throughput will not necessarily benefit from use of smaller particles.

In choosing a model to analyse performance it is not satisfactory to simplify the adsorption isotherm to a linear or rectangular form. Of single-step kinetic models, a pore diffusion model represents the BSA + DEAE-Vistec system better than a lumped mass transfer model. A two-step model, however, is likely to perform better still since pore diffusion is not completely rate-limiting.

SYMBOLS

c protein concentration in liquid, kg/m^3

c_f protein feed concentration in liquid, kg/m^3

c_i^j protein concentration in ith section of a pore at jth time increment, kg/m^3

c_l protein concentration in liquid between particles in lth section of column, kg/m^3

c^* protein concentration in pore (intra-particle) liquid in equilibrium with q, kg/m^3

c_o protein concentration in the liquid eluting from the column oulet, kg/m^3

$\mathcal{D}$ effective diffusivity of protein in pores, m^2/s

d_p particle diameter, m

F volumetric flow-rate of liquid through column, m^3/s

G pseudo-density of solid phase of adsorbent (dry weight per swollen bulk volume), kg/m^3

I ionic (added NaCl) concentration, kg/m^3

K_m Langmuir constant (ratio of adsorption and desorption rate constants), m^3/kg

k overall mass transfer coefficient, $m^3/(kg\ s)$

l column section

n number of elemental sections in a pore = $d_p/(2\Delta y)$

n_c number of elemental sections in column

q mass of protein per unit mass of dry adsorbent, kg/kg

q_m Langmuir constant (adsorption capacity), kg/kg

R rate of transfer of protein from extra-particle liquid to adsorbent in column section l, kg/s

r distance from centre of particle, m

s total area of pore mouth in an elemental section Δv of the column, m^2

t time, s

Δt time increment defined by eqn. 4, s

t_M liquid holdup time in the bed, s

u superficial velocity of liquid, m/s

Δv volume of elemental section of column, m^3

W dry mass of the ion exchanger, kg

y distance into pore from mouth, m

Δy length of elemental section of pore, m

ε void fraction of bed (extra-particle voidage/bulk volume)

ϕ pore fraction of bed (intra-particle pore volume/bulk volume)

REFERENCES

1 M. D. Rankin, in R. A. Grant (Editor), *Applied Protein Chemistry*, Applied Science Publishers, Essex, 1980, Ch. 6, pp. 169–180.
2 D. T. Jones, *Process Biochem.*, 9, No. 19 (1974) 17.
3 D. T. Jones, in G. G. Birch, K. J. Parker and J. F. Morgan (Editors), *Food from Waste*, Applied Science Publishers, 1976, Ch. 17. p. 242.
4 D. Halliday, *Process Biochem.*, 10, No. 4 (1975) 11.
5 E. J. Cohn, L. E. Strong, W. L. Hughes, D. J. Mulford, J. N. Ashworth, M. Merlin and H. L. Taylor, *J. Am. Chem. Soc.*, 68 (1946) 459.
6 E. J. Cohn, W. L. Hughes and J. H. Weare, *J. Am. Chem. Soc.*, 69 (1947) 1753.
7 J. M. Curling, L. O. Lindquist and S. Erikson, *Process Biochem.*, 12 (1977) 22.
8 J. M. Curling, J. Berglof, L. O. Lindquist and S. Erikson, *Vox Sang.*, 33 (1977) 97.
9 J. M. Curling, in R. Epton (Editor), *Chromatography of Synthetic and Biological Polymers*, Ellis Horwood, Chichester, 1978, Ch. 6.
10 J. M. Curling, in J. M. Curling (Editor), *Methods of Plasma Protein Chromatography*, Academic, London, 1980, pp. 77–91.
11 J. Saint-Blanchard, J. M. Kirzin, P. Riberon, F. Petit, J. Fourcart, P. Girot and C. Boscetti, in T. C. J. Gribnau, J. Visser and R. J. F. Nivard (Editors), *Affinity Chromatography and Related Techniques*, Elsevier, Amsterdam, 1982, p. 305.
12 J. Travis, J. Bowen, D. Tewkesbury, D. Johnson and R. Pannell, *J. Biochem.*, 157 (1976) 301.
13 R. Hanford, W. d'A. Maycock and L. Vallet, in R. Epton (Editor), *Chromatography of Synthetic and Biological Polymers*, Ellis Horwood, Chichester, 1978, Ch. 23.
14 J. L. Tayot, M. Tardy, P. Gattel, R. Plan and M. Roumiantzeff, in R. Epton (Editor), *Chromatography of Synthetic and Biological Polymers*, Ellis Horwood, Chichester, 1978, Ch. 8.
15 J. C. Janson and P. Hedman, *Adv. Biochem. Eng.*, 25 (1982) 43.
16 G. Leaver, J. R. Conder and J. A. Howell, *Sep. Sci. Technol.*, 22 (1987) 2037.
17 H. A. Chase, *J. Chromatogr.*, 297 (1984) 179.
18 P. D. G. Dean, W. S. Johnson and F. A. Middle, *Affinity Chromatography*, IRL Press, Oxford, 1985, Ch. 4.
19 J. P. Hamman and G. J. Calton, *(ACS Symposium Series*,

No. 271), American Chemical Society, Washington, DC, 1985, p. 105.

20 F. H. Arnold, J. J. Chalmers, M. S. Saunders, M. S. Croughan, H. W. Blanch and C. R. Wilke, (*ACS Symposium Series*, No. 271), American Chemical Society, Washington, DC, 1985, p. 113.

21 E. E. Graham and C. F. Fook, *AIChE J.*, 28 (1982) 245.

22 H. S. Tsou and E. E. Graham, *AIChE J.*, 31 (1985) 1959.

23 J. R. Conder, G. Leaver and J. A. Howell, *Inst. Chem. Eng. Symp. Ser.*, No. 118 (1990) 1.

24 C. Tien and G. Thodos, *Chem. Eng. Sci.*, 13 (1960) 120.

25 J. R. Conder and J. H. Purnell, *Trans. Faraday Soc.*, 65 (1969) 824.

26 B. J. Horstmann and H. A. Chase, *Chem. Eng. Res. Des.*, 67 (1989) 243.

27 F. H. Arnold, H. W. Blanch and C. R. Wilke, *Chem. Eng. J.*, 30 (1985) B25.

28 J. P. van der Wiel and J. A. Wesselingh, in A. E. Rodrigues, M. D. Levan and D. Tondeur (Editors), *Adsorption, Science and Technology*, Kluwer, Dordrecht, 1989.

29 T. W. Weber and R. K. Chakravorti, *AIChE J.*, 20 (1974) 228.

30 N. K. Hiester and T. Vermeulen, *Chem. Eng. Prog.*, 48 (1952) 505.

31 R. G. Lee and T. W. Weber, *Can. J. Chem. Eng.*, 47 (1969) 54.

32 M. E. Young, P. A. Carroed and R. L. Ball, *Biotech. Bioeng.*, 22 (1980) 947.

33 R. V. Dove, personal communication, 1982.